

LatentMove: Towards Complex Human Movement Video Generation

Ashkan Taghipour

The University of Western Australia

Morteza Ghahremani

Technical University of Munich

Mohammed Bennamoun

The University of Western Australia

Farid Boussaid

The University of Western Australia

Aref Miri Rekavandi

The University of Western Australia

Zinuo Li

The University of Western Australia

QiuHong Ke

Monash University

Hamid Laga

Murdoch University

Abstract

Image-to-video (I2V) generation seeks to produce realistic motion sequences from a single reference image. Although recent methods exhibit strong temporal consistency, they often struggle when dealing with complex, non-repetitive human movements, leading to unnatural deformations. To tackle this issue, we present LatentMove, a DiT-based framework specifically tailored for highly dynamic human animation. Our architecture incorporates a conditional control branch and learnable face/body tokens to preserve consistency as well as fine-grained details across frames. We introduce Complex-Human-Videos (CHV), a dataset featuring diverse, challenging human motions designed to benchmark the robustness of I2V systems. We also introduce two metrics to assess the flow and silhouette consistency of generated videos with their ground truth. Experimental results indicate that LatentMove substantially improves human animation quality—particularly when handling rapid, intricate movements—thereby pushing the boundaries of I2V generation. The code, the CHV dataset, and the evaluation metrics will be available at <https://github.com/--->.

1. Introduction

Human-centric image-to-video (I2V) models receive a single reference image as input and generate a temporally coherent video sequence conditioned on that reference frame.

Existing human-centric I2V models exhibit significant limitations in synthesizing realistic human actions, particularly those involving rapid transitions, intricate body dynamics, and abrupt pose changes (see Figure 1). These challenges often manifest as motion artifacts, deformations, or physically implausible sequences. To mitigate these issues, recent advances have focused mainly on integrating explicit motion control signals—such as skeleton pose, depth maps, segmentation maps, and surface normal maps—into I2V architectures [11, 21, 70]. These structured motion representations are crucial priors that constrain the generated motion trajectories. By incorporating these signals through specialized network modules, I2V models gain the ability to synthesize high-fidelity human motion sequences that adhere more faithfully to the underlying kinematics and physical constraints.

I2V backbone architectures predominantly follow two distinct paradigms: (i) *UNet-based architectures*, commonly referred to as Diffusion UNet, and (ii) *Transformer-based architectures*, known as DiT. UNet-based architectures can be further categorized into two groups. The first group builds upon UNet-based image generation backbones. These methods first train spatial components on human image generation tasks before involving temporal layers in the ultimate model, which are taught separately on image sequences (frames) [14]. A two-stage training process, however, is computationally demanding and often results in temporal inconsistency across frames. The second group integrates temporal modeling directly into the UNet

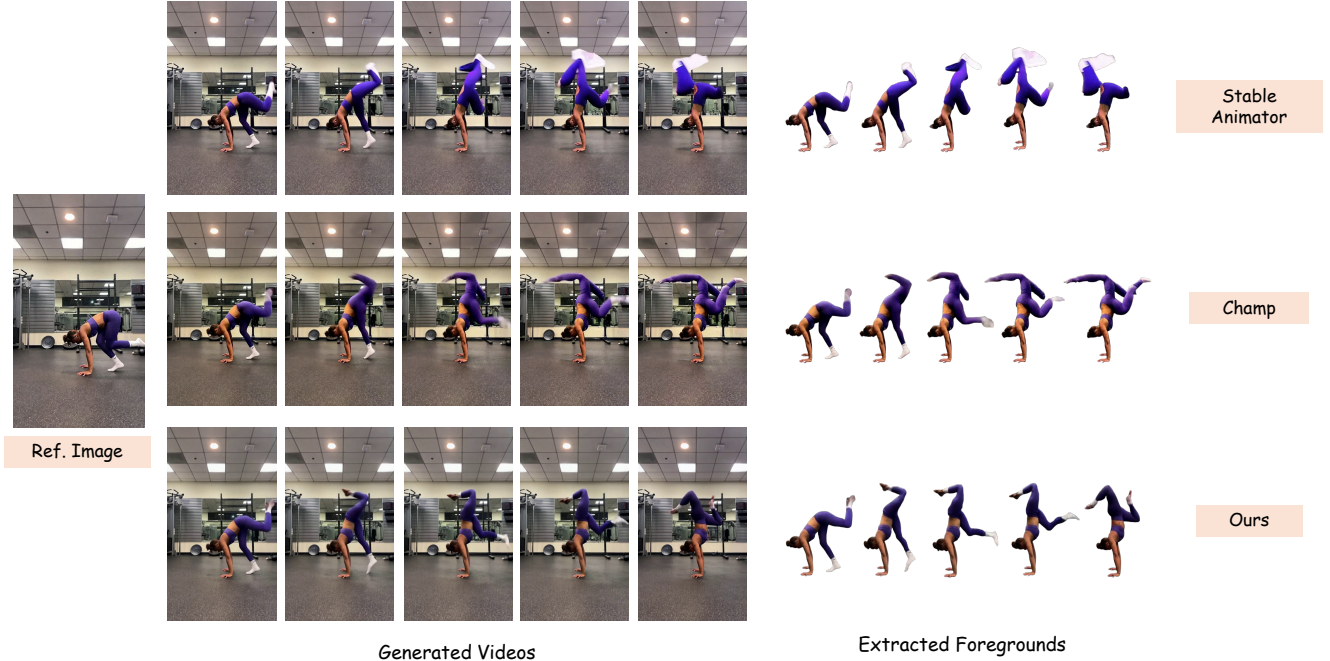


Figure 1. LatentMove is built on a well-established DiT backbone, featuring a DiT-specific condition encoder and learnable tokenization of face and body features to preserve motion consistency and fine-grained details across frames. Video files are provided in the Supplementary Materials.

backbone, enabling end-to-end training in a single stage [2]. This approach is computationally more efficient and better suited for video synthesis. However, due to inherent architectural limitations of the UNet design, these models struggle to generate long-range video sequences (e.g., exceeding 25 frames), leading to degradation in motion continuity and temporal coherence. To address the limitations of UNet-based architectures, DiT backbones have gained attention for their scalability [8], ability to capture long-range dependencies [32, 60], and flexibility in text conditioning [46]. While some recent studies [55, 62] have improved DiT models for text-to-video (T2V) generation, their potential for I2V human animation remains largely unexplored.

In this work, we adapt the CogVideoX I2V model [61] to generate complex movement human-centric video using depth conditioning signals, leveraging the strengths of DiT architectures to improve motion quality and temporal consistency. Unlike existing approaches that focus on structured and repetitive motions from datasets like the TikTok dance dataset [23] (which often lack dynamic and high-energy movements), LatentMove can generate more complex and diverse actions. In contrast to the use of CLIP image embeddings [33], which offer limited fine-grained facial and body consistency, LatentMove leverages DinoV2 [31] features and introduces learnable tokenization to enhance the aesthetic quality of generated videos. In short,

the contributions of our study are as follows:

- **DiT-Specific Condition Encoder:** We propose a novel condition encoder block tailored for DiT-based I2V networks, incorporating dedicated face and body encoder modules to improve human consistency in challenging movements.
- **Learnable Face & Body Tokens:** We propose learnable face and body tokens, initially derived from DinoV2 [31] features. These tokens are further refined using a cross-attention module and a body mask loss to enhance motion consistency in generated videos.
- **Automated Data Pipeline & Benchmark Dataset:** We develop an automated data pipeline for downloading, masking, depth extraction, and curating complex human movements. We also introduce Complex-Human-Videos (CHV), a dataset of 342 videos with diverse and intricate human motions, comparable in scale to the TikTok dance dataset [23].
- **Dedicated Evaluation Metrics for Video Content:** To evaluate motion consistency, we introduce two novel metrics—Dynamic Flow Consistency Index (DFCI) and Silhouette Consistency—designed to measure spatial and temporal coherence in human-centric generated videos.

2. Related Work

Video generation. Recent advancements in generative AI [25, 37, 39, 63, 69] have contributed to the development of video synthesis techniques, with methods like GANs [3, 51], VQ-VAE Transformers [24, 44, 50, 57], and diffusion models [1, 5, 6, 10, 15] improving both video quality and temporal consistency. Video synthesis is mainly categorized into T2V [5, 16] and I2V [27, 40, 68], with I2V focused on predicting future frames from a reference image. To improve control in I2V, methods integrate conditions like audio [29], camera control [17], scene layout [9], human body features [45, 53, 70], and motion synthesis [67].

Condition-Guided Human Animation. Human image animation has seen substantial progress, particularly with networks that extract diverse human-related features, including skeleton pose [59], dense pose [12], depth [58], body part segmentation [26], and normal maps. Early works [22, 35] employed GANs for animating humans in reference images but often resulted in artifacts. Disco [48] pioneered the use of diffusion models for human animation; however, it struggled with generating consistent human body parts. AnimateAnyone [20] addressed character inconsistency by incorporating ReferenceNet into the 2D UNet backbone but faced challenges with misalignment between pose sequences and generated frames. AnimateAnyone 2 [21] introduced human-object interactions but, like its predecessor, remains closed-source. MagicAnimate [56] utilized DensePose [12] as a conditioning signal to reduce body misalignment. Champ [70] further addressed misalignment by incorporating depth maps, masks, and normal maps. Despite these improvements, temporal consistency remained a challenge, as these methods relied on 2D UNet-based diffusion models, requiring separate training stages for spatial and temporal components.

VividPose [47], UniAnimate [49], MimicMotion [66], and others [4, 28, 30, 41] adopted a temporally-equipped 3D UNet architecture, enabling single-stage training for more consistent and well-aligned human animations. Additionally, they leveraged the CLIP image encoder to extract reference image features to improve body and face consistency in the generated frames. ControlNetX [32] introduced an efficient control branch within a 3D UNet architecture to enhance human image animation. StableAnimator [42] further improved facial consistency by incorporating a dedicated face module and a face mask loss into the 3D UNet framework. Despite these advancements, these methods remain constrained by UNet-based architectures, which, though effective, lack scalability and struggle to capture long-range dependencies [8].

Recently, DiT-based architectures have emerged as a promising alternative, offering enhanced scalability and superior global context modeling [16, 27, 61]. EasyAnimate [55] introduced pose control within a T2V DiT frame-

work but lacks support for I2V human animation. Human-DiT [11] integrates DiT with pose control, focusing primarily on long video continuation utilizing significant computational resources with 128 H100 GPUs for training.

Building upon these advancements, we adapt the CogVideoX DiT-based I2V model [61] to generate complex human movement videos. Specifically, the DiT-specific condition encoder is designed to inject depth condition signals into the DiT block, while the learnable face and body tokens, along with the body mask loss, are tailored to maintain consistency in facial and body movements. These innovations collectively enhance the generation of complex human-centric videos, ensuring more coherent and realistic motion in challenging scenarios.

3. Proposed Method

LatentMove generates a human-centric video of L color frames with height H and width W , denoted as $\mathbf{V} \in \mathbb{R}^{L \times H \times W \times 3}$, by animating the reference image I_r in alignment with conditional signals $\mathcal{C}^{1:L}$. To enable efficient sampling and reconstruction, a 3D VAE [18, 61] ($\mathcal{D}(\mathcal{E}(\cdot))$) encodes video frames in a latent space with C channels $\mathbf{z} \in \mathbb{R}^{L/k \times C \times h \times w}$, where $h \ll H$ and $w \ll W$, and k denotes the temporal kernel size that compresses each k sequential frames into one in the latent space. The loss function is defined as:

$$\mathcal{L} = \mathbb{E}_{\mathbf{z}, \mathbf{x}, \mathbf{y}, \epsilon \sim \mathcal{N}(\mathbf{0}, \mathbf{I})} [\|\epsilon - \epsilon_{\theta}(\mathbf{z}_t, t, \eta_{\theta}(x), \tau_{\theta}(y))\|_2^2], \quad (1)$$

where $\tau_{\theta}(\cdot)$ is a text encoder for input text y and $\eta_{\theta}(\cdot)$ denotes the learnable condition encoder in our learnable branch with user input $x = \{\mathcal{C}^{1:L}, I_r\}$. Given x , the generated frames must maintain character consistency, particularly in facial features and body outfit, while ensuring motion aligns with the provided condition signals.

The proposed framework is shown in Fig. 2. The LatentMove model has three key components: *i) Face-Body (FB) Encoder* introduces a face-body encoder to extract face and body tokens from the given reference image; *ii) Condition Encoder*, which integrates the FB tokens and conditional signals via a patch embedder suitable for injection into the learnable DiT blocks; *iii) Diffusion Transformer (DiT)* serves as the diffusion branch with frozen layers, receiving text tokens \mathbf{z}_{text} and the latent encoding of input frames \mathbf{z}_f . It interacts with its trainable counterpart in the ControlNet branch to generate a sequence of processed frames in the latent space. *Notation:* We define B as batch size, C as VAE channels, f_{em} as the embedding size of the DiT feature, h and w as latent encoding dimensions, and L as the length of the condition signals.

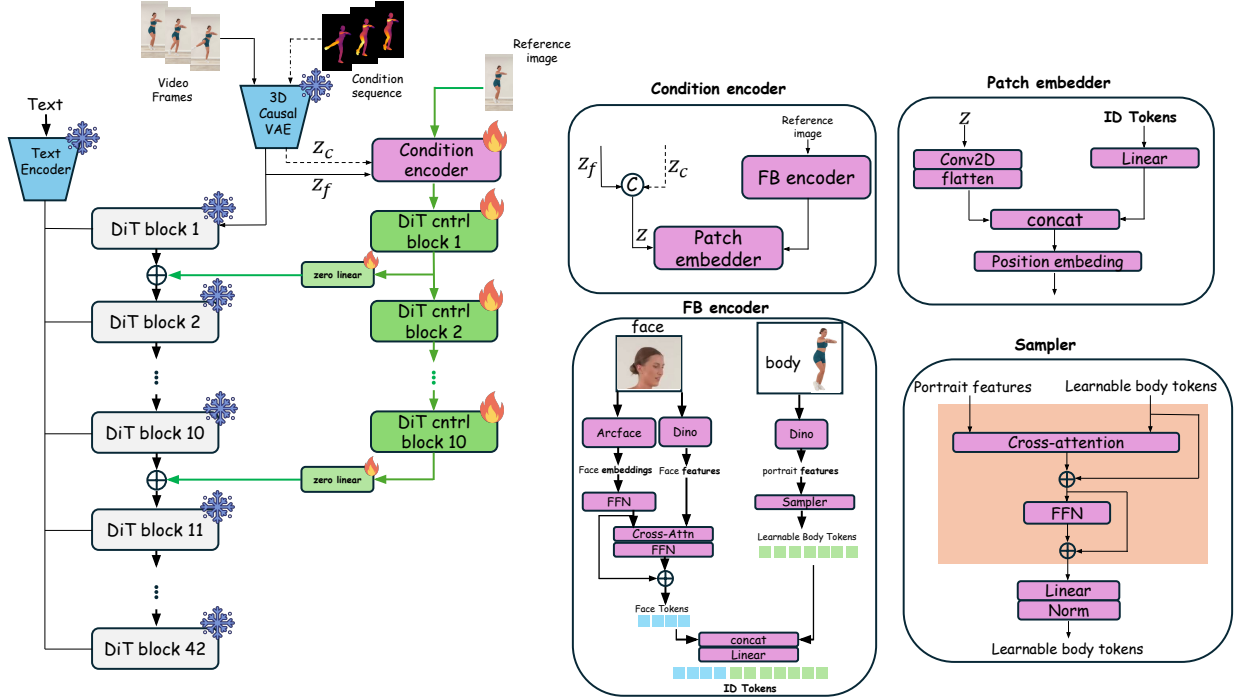


Figure 2. Training framework of LatentMove. The input frame and the condition sequences are processed through a 3D spatial-temporal VAE to produce latent encodings. The Face-Body (FB) encoder extracts body and face tokens, which are then combined with the latent encodings by the Condition encoder. While the main branch DiT remains frozen, we train the conditional network using a ControlNet and add it to the DiT blocks via zero linear modules.

3.1. Condition Encoder

The Condition Encoder’s role is to integrate the latent representation of the input frames and the condition signal, preparing them for seamless use in the ControlNet branch. To achieve this, we apply the 3D Causal VAE with frozen weights [18, 61] to progressively compress the input video tensor with size $\mathbf{V} \in \mathbb{R}^{B \times L \times H \times W \times 3}$ into a compact latent representation of the size $z_f \in \mathbb{R}^{B \times C \times L/k \times h \times w}$, where k is the temporal kernel size.

Likewise, we process the condition signals through the frozen 3D Causal VAE to obtain its compressed encoding z_c . Encoding both the condition signals and video frames within the same latent space ensures coherent interactions between their latent representations (Fig. 3). The latent encodings z_f and z_c are concatenated, mapped into f_{em} channels and flattened into the shape $\mathbf{z} \in \mathbb{R}^{B \times (L/k)hw \times f_{em}}$. As detailed in the subsequent section, the Face-Body (FB) encoder generates N tokens, each with a feature embedding of size f_{em} . These tokens are then concatenated with the latent encodings along the spatial-temporal dimension, yielding $\mathbf{z} \in \mathbb{R}^{B \times ((L/k)hw + N) \times f_{em}}$. We concatenate three encodings to ensure that the feature embedding of each model is preserved during computation. To further en-

hance temporal-spatial position awareness, we employ 3D RoPE [38, 61] for positional encoding.

3.2. Face-Body (FB) Encoder

As illustrated in the framework figure 2, the FB encoder is a trainable module designed to maintain the consistency of fine-grained human-related contents between the reference image I_r and the generated frames. To achieve this, we focus on two key human-centric features: the body and the face/head. The core design involves extracting tokens from body and facial patches, selecting the most relevant ones, and stacking them before feeding them into the patch embedder (Sec. 3.3).

Body Encoder: The high-level features of the masked body (including the head) are first extracted using the frozen DINOv2 image encoder [31]. Unlike traditional techniques [42, 49, 66, 70], which encode the entire reference image into a single token using CLIP [33], we use DINOv2 [31] image encoder that consider local regions. DINOv2 encodes local features by partitioning the reference image into 14×14 patches, resulting in N_{dino} tokens of length f_{dino} . It is important to note that while CLIP jointly learns from both images and text to align these modalities, DINOv2 operates solely within the visual domain, providing a more robust

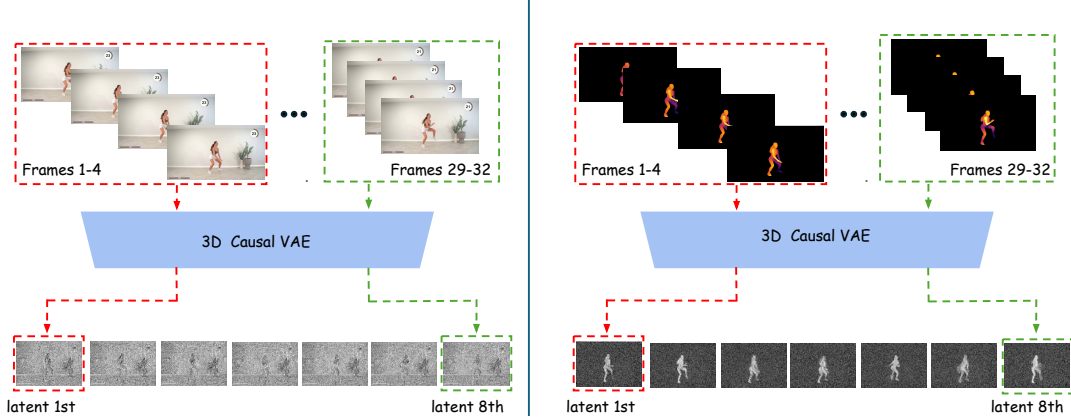


Figure 3. Illustration of the 3D VAE compressing four frames into a single latent representation. Unlike UNet-based models, which do not compress the temporal dimension, conditions must be mapped to the latent space for proper alignment.

representation of visual data. A considerable portion of the N_{dino} tokens may be related to the background, so we exclude those from our computations using a Sampler. The objective of the Sampler is to select the relevant n body tokens while discarding unimportant tokens like background, i.e. $n \ll N_{dino}$. As illustrated in Fig. 2, the Sampler first maps the extracted DINOv2 features (\mathbf{D}) into f_{em} channels and then incorporates a cross-attention module where the keys and values are the DINOv2 tokens, while the query consists of n trainable body tokens of size f_{em} :

$$\mathbf{Q} = \text{nn.parameter}(\mathbf{0}_{n \times f_{em}}) \quad (2)$$

$$\mathbf{K} = \mathbf{D}\mathbf{W}_K, D \in \mathbb{R}^{N_{dino} \times f_{em}} \quad (3)$$

$$\mathbf{V} = \mathbf{D}\mathbf{W}_V, D \in \mathbb{R}^{N_{dino} \times f_{em}} \quad (4)$$

Then cross-attention is computed via:

$$\text{top}_n(\mathbf{D}) = \text{softmax}\left(\frac{\mathbf{Q}\mathbf{K}^T}{\sqrt{f_{em}}}\right)\mathbf{V}. \quad (5)$$

The rectified tokens are then passed through a feedforward network (FFN) and normalized to produce learnable body tokens. As discussed later, we employ a mask loss that emphasizes the human body (as the foreground) to guide the Sampler in accurately selecting the most relevant token set from the initially extracted DINOv2 tokens.

Face Encoder: Compared to the body, the facial region occupies a smaller area, leading to less effective backpropagation for facial features. Moreover, even minor discrepancies in facial characteristics can significantly impact aesthetic quality. To address this, we introduce a dedicated encoder for the facial region. The process of extracting tokens from the face is illustrated in Fig. 2. We employ ArcFace [7] to extract a global feature embedding for the facial region and then map it into f_{em} channels. Similar to the body, we also use DINOv2 to capture fine-grained facial details

over the cropped facial area and then map them into feature embeddings of f_{em} . To identify the most relevant DINO features (\mathbf{K}_{local} and \mathbf{V}_{local}) in relation to the global embedding (\mathbf{Q}_{global}), we apply cross-attention, expressed as:

$$\mathbf{A}_{facial} = \text{softmax}\left(\frac{\mathbf{Q}_{global}\mathbf{K}_{local}^T}{\sqrt{f_{em}}}\right)\mathbf{V}_{local}^T. \quad (6)$$

At the final stage of the FB module, the face tokens are concatenated with the body tokens to form the ID token, which encapsulates the aesthetic features of the reference image.

3.3. Frozen DiTs

The CogVideoX series [18, 61] introduces a set of DiT blocks that serve as the backbone of their models. In particular, the CogVideoX [61] 5-billion-parameter architecture comprises 42 sequential DiT blocks. However, in this study, we keep these blocks frozen and instead train the condition branch using ControlNet [64] on the first 10 DiT blocks.

3.4. Loss Criterion

LatentMove is designed to enhance motion fidelity in human-centric content while maintaining high aesthetic quality, particularly in the generation of human features. To achieve this, we guide the diffusion process to prioritize human regions by defining a human mask \mathbf{m} . This refinement ensures that the model focuses on preserving the dynamics of human motion and structural consistency. Hence, we modify the loss function in Eq. 1 as follows:

$$\mathcal{L} = \mathbb{E}_{\mathbf{z}, \mathbf{x}, \mathbf{y}, \epsilon \sim \mathcal{N}(\mathbf{0}, \mathbf{I})} [||(\epsilon - \epsilon_\theta(\mathbf{z}_t, t, \eta_\theta(x), \tau_\theta(y)) \odot (1 - \mathbf{m}))||_2^2] + \lambda \mathbb{E}_{\mathbf{z}, \mathbf{x}, \mathbf{y}, \epsilon \sim \mathcal{N}(\mathbf{0}, \mathbf{I})} [||(\epsilon - \epsilon_\theta(\mathbf{z}_t, t, \eta_\theta(x), \tau_\theta(y)) \odot \mathbf{m})||_2^2], \quad (7)$$

where $\lambda \geq 1$ denotes a predetermined body-mask guidance hyperparameter enhances the importance of human-centric regions in the loss computation.

4. Experiments

Datasets and Evaluation setup. We trained our network using two distinct datasets. The first is the widely recognized TikTok dataset [23], which consists of 340 videos. Additionally, we curated our own dataset, Complex-Human-Videos (CHV), from various online sources. CHV comprises 300 videos featuring complex human movements such as jumping, kicking, rotating, and gymnastics, along with 42 validation videos. A comparison between CHV and the TikTok dataset is provided in Section 3 of the Supplementary Material, highlighting CHV’s more intricate motion patterns and diverse human gestures.

Implementation Details and competing methods. In our experiments, we used DepthAnything-v2 [58] for depth extraction as conditioning sequences (the background is discarded using SAM-v2 [34]). We also employed ArcFace [7] for extracting facial features. The entire trainable network was trained from scratch, including the ten DiT blocks in the ControlNet branch and other trainable modules. The training was carried out for 20K steps on three NVIDIA H100 GPUs, with a batch size of 24, a learning rate of 1×10^{-5} , 500 warm-up steps, and $\lambda = 4$. We compared our method to recent human animation models, including the GAN-based approach MRAA [36] and several diffusion models such as DisCo [48], [56] AnimateAnyone [20], Champ [70], Unanimate [49], MimicMotion [66], ControlNeXt [32], and StableAnimator [42].

4.1. Proposed metrics for evaluation of generated human-centric videos

Existing metrics, such as FVD [43], LPIPS [65], SSIM [52], PSNR [19], CSIM [13], and L1, focus primarily on evaluating the quality of the individual frame of a sequence without considering their temporal interactions. In the case of time-series data, metrics are needed to precisely assess how well video generated captures complex motion dynamics and pose transitions over time. This gap has led to the development of two novel metrics introduced in this work, designed to evaluate both the spatial and temporal aspects of generated videos, as described in the following.

Dynamic Flow Consistency Index (DFCI). This metric assesses consistency in optical flow—representing both the direction and speed of motion—to characterize the motion of human-centric data across consecutive generated frames. We evaluated the reliability and consistency of flow vectors \mathbf{O} in short and long terms T . DFCI indicates that the motion of humans in the generated frames \mathbf{O}_{gen} closely resembles

and accurately reflects the true motion dynamics \mathbf{O}_{gt} :

$$\text{DFCI}(V, T) = \frac{1}{2(L - T)} \sum_{t=T}^L |\mathbf{O}_{gt}(V, t, t - T) - \mathbf{O}_{gen}(V, t, t - T)|. \quad (8)$$

$\mathbf{O}(V, t, t - T)$ denotes the optical flow of video V between frames t and $t - T$ along x and y axes. In this study, we used UniMatch [54] to predict frames’ optical flow. Smaller T s (such as ‘ $T = 1$ ’, which is denoted as T_1 hereafter) indicate that only the immediate consecutive frames are considered for flow consistency, which is suitable for short-term dynamics. Larger T s (e.g., T_4 and T_5) consider flow over a wide range of frames, providing a long-term flow consistency. Due to the importance of human-centric data, we applied these metrics to both human-centric data with and without background. The human contents are segmented as the foreground, while non-human regions are labeled as the background in the ground truth and generated video frames. The ideal value for DFCI is zero, which means that there is no motion conflict between the ground truth and the generated videos. More details are provided in Sec. 1 of Supplementary Material.

Silhouette Consistency: This metric assesses the degree to which the shapes of segmented human-centric objects (foreground silhouettes) are preserved across frames in generated frames. It evaluates these silhouettes’ spatial and temporal coherence, providing insights into the consistency and reliability of human-centric representations over time (frames). The Dice score is calculated across the corresponding frames to compute this metric, and the average result is reported here.

4.2. Experiments with TikTok

In this experiment, we trained our network exclusively on the TikTok dataset [23] and evaluated its performance using the same TikTok validation samples as prior works [32, 42, 48, 56, 70], ensuring a fair comparison with existing approaches. The assessment results are presented in Table 1. The proposed method outperforms all compared SOTA approaches in most metrics, including L1, SSIM, LPIPS, and FVD, indicating improved perceptual quality, structural similarity, and temporal coherence in generated videos. Our results are comparable to SOTA methods for the remaining metrics, including PSNR, PSNR*, and CSIM, considering that no single approach achieves the best performance across all metrics.

4.3. Experiments with CHV

In the CHV dataset, we re-trained the top three state-of-the-art (SOTA) models from Table 1 in our dataset. Among them, Champ [70] was originally trained on multiple conditioning signals, including pose, depth, normal maps, and

Table 1. Performance comparison of models on TikTok validation dataset. Note that all models are trained on the TikTok training set.

Model	Venue	L1 (E-4)↓	PSNR [19]↑	PSNR* [48]↑	SSIM↑	LPIPS↓	CSIM [13]↑	FVD↓
MRAA [36]	CVPR 2021	3.21	-	18.14	0.672	0.296	0.248	284.82
DisCo [48]	CVPR 2024	3.78	29.03	16.55	0.668	0.292	0.315	292.80
MagicAnimate [56]	CVPR 2024	3.13	29.16	-	0.714	0.239	0.462	179.07
AnimateAnyone [20]	CVPR 2024	-	29.56	-	0.718	0.285	0.457	171.90
Champ [70]	EECV 2024	2.94	29.91	-	0.802	0.231	0.350	160.82
Unianimate [49]	Arxiv 2024	2.66	30.77	20.58	0.811	0.231	0.479	148.06
MimicMotion [66]	Arxiv 2024	5.85	-	14.44	0.601	0.416	0.262	326.57
ControlNeXt [32]	Arxiv 2024	6.20	-	13.83	0.615	0.416	0.360	326.57
StableAnimator [42]	CVPR 2025	2.87	30.81	20.66	0.801	0.232	0.831	<u>140.62</u>
LatentMove (ours)		2.62	<u>30.79</u>	<u>20.63</u>	<u>0.804</u>	0.230	<u>0.798</u>	139.2

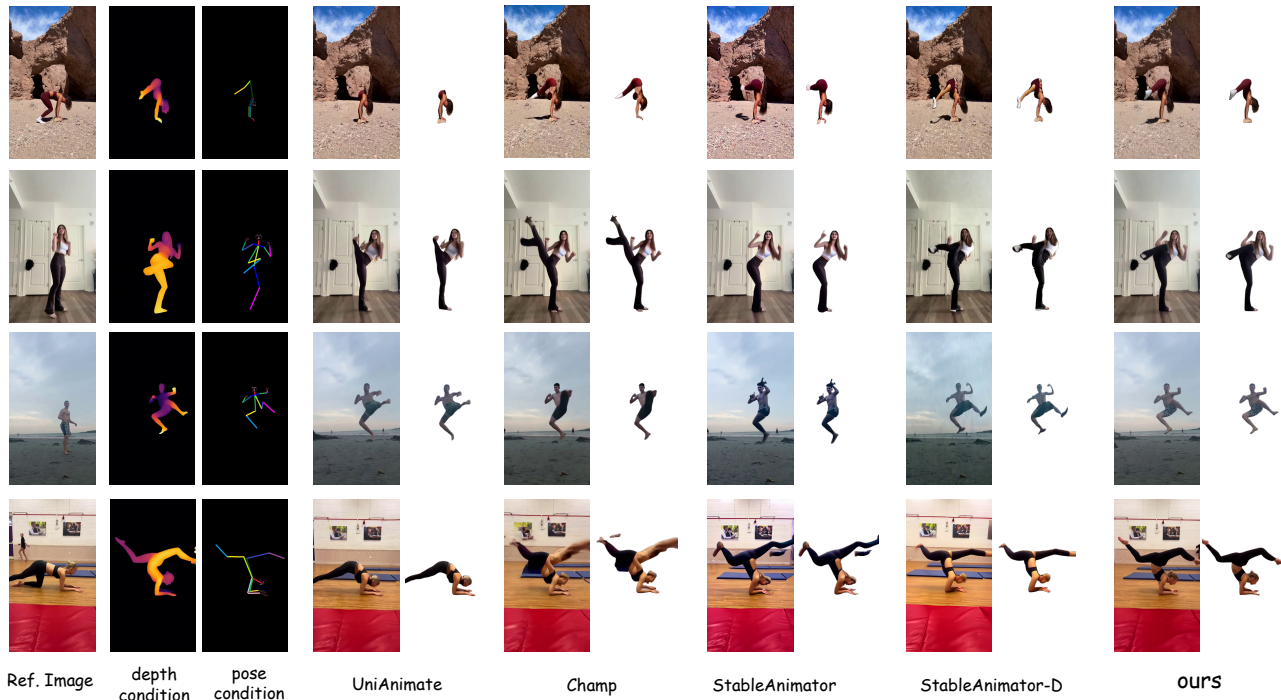


Figure 4. Visualization of results from different methods on the CHV dataset, with highlighted masked human regions.

masks. In contrast, the other two SOTA models, i.e. UniAnimate [49] and StableAnimator [42], were trained solely on human skeletons. To ensure that our performance gains are not solely due to the choice of conditioning input but also stem from architectural innovations, we conducted an additional experiment. Specifically, we re-trained StableAnimator [42] with depth maps as the conditioning input, referring to this variant as StableAnimator-D. The evaluation results for these models are presented in Table 2. We assess their performance using two newly proposed evaluation metrics: DFCI and silhouette consistency.

Table 2 reveals that DFCI scores for videos with backgrounds are significantly lower than those without backgrounds, suggesting that the optical flow of human-centric content must be analyzed separately in human-focused

video generation. Furthermore, the table indicates that motion discrepancy is substantially higher in long-range motion sequences compared to short-range ones. When considering both short- and long-term motion consistency, as well as background variations, LatentMove achieves the highest overall performance. However, the results also suggest areas for further improvement. Silhouette consistency measures the persistence of human-centric structures across generated frames. LatentMove achieved 83.8% in silhouette consistency, which is about 4% higher than StableAnimator-D, indicating that it better preserves human content throughout the generated video sequences. Figure 4 compares our method with SOTA approaches, highlighting superior condition binding, especially for complex human gestures. Existing methods struggle with accurate condi-

Table 2. Comparison of different models on the CHV dataset using the proposed DFCI and silhouette consistency metrics.

Model	DFCI w/o background↓					DFCI w/ background↓					Silhouette
	T_1 (short-term)	T_2	T_3	T_4	T_5 (long-term)	T_1	T_2	T_3	T_4	T_5	Consistency↑
UniAnimate [49]	4.70	8.25	10.62	13.4	14.21	1.15	1.95	2.68	3.36	3.9	0.724
Champ [70]	4.25	6.66	8.29	10.03	11.10	0.95	1.53	2.07	2.39	2.67	0.755
StableAnimator [42]	4.36	7.40	9.23	11.32	12.29	1.02	1.69	2.28	2.74	3.10	0.745
StableAnimator w/ depth	4.11	6.52	8.15	9.94	10.85	0.89	1.47	2.00	2.32	2.64	0.794
LatentMove (ours)	3.82	5.95	7.04	8.18	9.16	0.66	1.06	1.48	1.73	1.93	0.838



Figure 5. Impact of ablating key components of our model. b) Performance comparison of our model with DinoV2 and CLIP. DinoV2 captures finer details, enhancing accuracy.

tioning: UniAnimate misses body parts, StableAnimator fails to bind conditions, and Champ shows inaccuracies. Depth-based conditioning improves StableAnimator, but issues persist. In contrast, LatentMove ensures precise condition adherence while maintaining shape and color consistency with the reference image. Additional multi-frame results are in Sec. 4 of Supplementary Material.

4.4. Ablation Study

We ablate the core modules of LatentMove—face encoder, body encoder, and mask loss—to evaluate their effectiveness. As reported in Table 3, removing each module increases DFCI (higher DFCI is worse), confirming their importance. The body encoder has the most significant impact, followed by mask loss, as both handle larger portions of the human body. In contrast, the face encoder affects a smaller region, leading to a smaller increase in DFCI. The silhouette consistency also reflects this, as the absence of the body encoder causes a significant drop, while the face encoder has the least impact. This is because we segment the image into foreground (human) and background regions, meaning facial details do not significantly affect silhouette consistency. Figure 5(a) presents a visual ablation of each core module. Removing the face or body encoder degrades face and body generation, respectively, while removing mask loss leads to misalignment between the generated body and the given condition.

We also assess the impact of using the DINOv2 image encoder instead of the widely-used CLIP in human animation [20, 32, 42, 49, 70], particularly for complex actions. As shown in Table 4, replacing our DINOv2’s learnable tokens with CLIP’s single-token degrades both DFCI and silhouette scores. This aligns with the visual results in Fig-

Table 3. Ablation study on different modules of LatentMove

Model	DFCI ↓	Silhouette
	T_1	Consistency↑
LatentMove w/o face Enc.	3.89	0.827
LatentMove w/o body Enc.	4.17	0.778
LatentMove w/o mask loss.	4.09	0.793
LatentMove w/ all modules	3.82	0.838

Table 4. Ablation study on different vision encoders

Model	DFCI ↓	Silhouette
	T_1	Consistency↑
LatentMove w/ CLIP	4.27	0.762
LatentMove w/ DinoV2	3.82	0.838

ure 5(b), where DINOv2 better preserves the alignment between the generated frame and the given condition. In contrast, CLIP retains global context but loses finer body alignments, likely because encoding the entire reference image into a single token lacks sufficient detail.

We explore three methods for injecting condition signals into CogVideoX, which uses a 3D VAE to compress four frames into a single latent representation (unlike traditional VAEs with a one-to-one mapping). Our results show that neither summing the 3D VAE latents of condition signals nor using ConvNets to inject them into the generated frames is effective (see Figure 6 and Supplementary Material-Sec. 2 for details). Instead, concatenating the 3D VAE latents of condition signals alongside frame latents yields the best results.

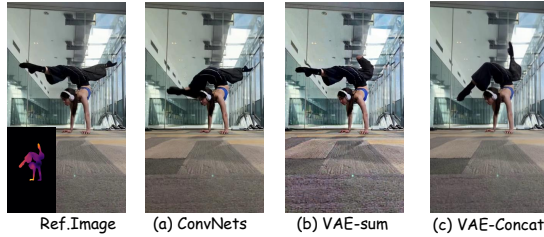


Figure 6. Comparison of 3D VAE compression (VAE-sum & concat) vs. non-compression (ConvNets) in spatial-temporal alignment.

5. Conclusion

This study explored the potential of DiTs for human-centric I2V. Our proposed method, LatentMove, introduced learnable face and body tokenization while leveraging depth as a conditioning signal via a DiT-specific condition encoder. LatentMove excels in generating videos with complex human movements, achieving strong qualitative results across the TikTok Dance and HCV datasets. While LatentMove demonstrated significant improvements in motion generation, our proposed DFCI and Silhouette Consistency metrics indicate areas for further refinement, particularly in enhancing human motion generation

References

- [1] Omer Bar-Tal, Hila Chefer, Omer Tov, Charles Herrmann, Roni Paiss, Shiran Zada, Ariel Ephrat, Junhwa Hur, Guanghui Liu, Amit Raj, et al. Lumiere: A space-time diffusion model for video generation. In *SIGGRAPH Asia 2024 Conference Papers*, pages 1–11, 2024. 3
- [2] Andreas Blattmann, Tim Dockhorn, Sumith Kulal, Daniel Mendelevitch, Maciej Kilian, Dominik Lorenz, Yam Levi, Zion English, Vikram Voleti, Adam Letts, et al. Stable video diffusion: Scaling latent video diffusion models to large datasets. *arXiv preprint arXiv:2311.15127*, 2023. 2
- [3] Tim Brooks, Janne Hellsten, Miika Aittala, Ting-Chun Wang, Timo Aila, Jaakko Lehtinen, Ming-Yu Liu, Alexei Efros, and Tero Karras. Generating long videos of dynamic scenes. *Advances in Neural Information Processing Systems*, 35:31769–31781, 2022. 3
- [4] Di Chang, Hongyi Xu, You Xie, Yipeng Gao, Zhengfei Kuang, Shengqu Cai, Chenxu Zhang, Guoxian Song, Chao Wang, Yichun Shi, et al. X-dyna: Expressive dynamic human image animation. *arXiv preprint arXiv:2501.10021*, 2025. 3
- [5] Hila Chefer, Uriel Singer, Amit Zohar, Yuval Kirstain, Adam Polyak, Yaniv Taigman, Lior Wolf, and Shelly Sheynin. Videojam: Joint appearance-motion representations for enhanced motion generation in video models. *arXiv preprint arXiv:2502.02492*, 2025. 3
- [6] Giannis Daras, Weili Nie, Karsten Kreis, Alex Dimakis, Morteza Mardani, Nikola Kovachki, and Arash Vahdat. Warped diffusion: Solving video inverse problems with image diffusion models. *Advances in Neural Information Processing Systems*, 37:101116–101143, 2025. 3
- [7] Jiankang Deng, Jia Guo, Niannan Xue, and Stefanos Zafeiriou. Arcface: Additive angular margin loss for deep face recognition. In *Proceedings of the IEEE/CVF Conference on Computer Vision and Pattern Recognition (CVPR)*, 2019. 5, 6
- [8] Kunyu Feng, Yue Ma, Bingyuan Wang, Chenyang Qi, Haozhe Chen, Qifeng Chen, and Zeyu Wang. Dit4edit: Diffusion transformer for image editing. *arXiv preprint arXiv:2411.03286*, 2024. 2, 3
- [9] Weixi Feng, Chao Liu, Sifei Liu, William Yang Wang, Arash Vahdat, and Weili Nie. Blobgen-vid: Compositional text-to-video generation with blob video representations. *arXiv preprint arXiv:2501.07647*, 2025. 3
- [10] Michael Fuest, Vincent Tao Hu, and Björn Ommer. Mask-flow: Discrete flows for flexible and efficient long video generation. *arXiv preprint arXiv:2502.11234*, 2025. 3
- [11] Qijun Gan, Yi Ren, Chen Zhang, Zhenhui Ye, Pan Xie, Xiang Yin, Zehuan Yuan, Bingyue Peng, and Jianke Zhu. Humandit: Pose-guided diffusion transformer for long-form human motion video generation. *arXiv preprint arXiv:2502.04847*, 2025. 1, 3
- [12] Rıza Alp Güler, Natalia Neverova, and Iasonas Kokkinos. Densepose: Dense human pose estimation in the wild. In *Proceedings of the IEEE conference on computer vision and pattern recognition*, pages 7297–7306, 2018. 3
- [13] Jianzhu Guo, Dingyun Zhang, Xiaoqiang Liu, Zhizhou Zhong, Yuan Zhang, Pengfei Wan, and Di Zhang. Liveportrait: Efficient portrait animation with stitching and retargeting control. *arXiv preprint arXiv:2407.03168*, 2024. 6, 7
- [14] Yuwei Guo, Ceyuan Yang, Anyi Rao, Zhengyang Liang, Yaohui Wang, Yu Qiao, Maneesh Agrawala, Dahua Lin, and Bo Dai. Animatediff: Animate your personalized text-to-image diffusion models without specific tuning. *arXiv preprint arXiv:2307.04725*, 2023. 1
- [15] Agrim Gupta, Lijun Yu, Kihyuk Sohn, Xiuye Gu, Meera Hahn, Fei-Fei Li, Irfan Essa, Lu Jiang, and José Lezama. Photorealistic video generation with diffusion models. In *European Conference on Computer Vision*, pages 393–411. Springer, 2024. 3
- [16] Yoav HaCohen, Nisan Chiprut, Benny Brazowski, Daniel Shalem, Dudu Moshe, Eitan Richardson, Eran Levin, Guy Shiran, Nir Zabari, Ori Gordon, et al. Ltx-video: Realtime video latent diffusion. *arXiv preprint arXiv:2501.00103*, 2024. 3
- [17] Hao He, Yinghao Xu, Yuwei Guo, Gordon Wetzstein, Bo Dai, Hongsheng Li, and Ceyuan Yang. Cameractrl: Enabling camera control for text-to-video generation. *arXiv preprint arXiv:2404.02101*, 2024. 3
- [18] Wenyi Hong, Ming Ding, Wendi Zheng, Xinghan Liu, and Jie Tang. Cogvideo: Large-scale pretraining for text-to-video generation via transformers. *The Eleventh International Conference on Learning Representations (ICLR 2023)*, 2023. 3, 4, 5

- [19] Alain Horé and Djemel Ziou. Image quality metrics: Psnr vs. ssim. In *2010 20th International Conference on Pattern Recognition*, pages 2366–2369, 2010. 6, 7
- [20] Li Hu. Animate anyone: Consistent and controllable image-to-video synthesis for character animation. In *Proceedings of the IEEE/CVF Conference on Computer Vision and Pattern Recognition*, pages 8153–8163, 2024. 3, 6, 7, 8
- [21] Li Hu, Guangyuan Wang, Zhen Shen, Xin Gao, Dechao Meng, Lian Zhuo, Peng Zhang, Bang Zhang, and Liefeng Bo. Animate anyone 2: High-fidelity character image animation with environment affordance. *arXiv preprint arXiv:2502.06145*, 2025. 1, 3
- [22] Zhichao Huang, Xintong Han, Jia Xu, and Tong Zhang. Few-shot human motion transfer by personalized geometry and texture modeling. In *Proceedings of the IEEE/CVF Conference on Computer Vision and Pattern Recognition*, pages 2297–2306, 2021. 3
- [23] Yasamin Jafarian and Hyun Soo Park. Learning high fidelity depths of dressed humans by watching social media dance videos. In *2021 IEEE/CVF Conference on Computer Vision and Pattern Recognition (CVPR)*, pages 12748–12757, 2021. 2, 6
- [24] Yuming Jiang, Shuai Yang, Tong Liang Koh, Wayne Wu, Chen Change Loy, and Ziwei Liu. Text2performer: Text-driven human video generation. In *Proceedings of the IEEE/CVF International Conference on Computer Vision*, pages 22747–22757, 2023. 3
- [25] Yang Jin, Zhicheng Sun, Ningyuan Li, Kun Xu, Hao Jiang, Nan Zhuang, Quzhe Huang, Yang Song, Yadong Mu, and Zhouchen Lin. Pyramidal flow matching for efficient video generative modeling. *arXiv preprint arXiv:2410.05954*, 2024. 3
- [26] Rawal Khirodkar, Timur Bagautdinov, Julieta Martinez, Su Zhaoen, Austin James, Peter Selednik, Stuart Anderson, and Shunsuke Saito. Sapiens: Foundation for human vision models. In *European Conference on Computer Vision*, pages 206–228. Springer, 2024. 3
- [27] Weijie Kong, Qi Tian, Zijian Zhang, Rox Min, Zuozhuo Dai, Jin Zhou, Jiangfeng Xiong, Xin Li, Bo Wu, Jianwei Zhang, et al. Hunyuanvideo: A systematic framework for large video generative models. *arXiv preprint arXiv:2412.03603*, 2024. 3
- [28] Hongxiang Li, Yaowei Li, Yuhang Yang, Junjie Cao, Zhihong Zhu, Xuxin Cheng, and Long Chen. Dispose: Disentangling pose guidance for controllable human image animation. *arXiv preprint arXiv:2412.09349*, 2024. 3
- [29] Gaojie Lin, Jianwen Jiang, Jiaqi Yang, Zerong Zheng, and Chao Liang. Omnihuman-1: Rethinking the scaling-up of one-stage conditioned human animation models. *arXiv preprint arXiv:2502.01061*, 2025. 3
- [30] Yifang Men, Yuan Yao, Miaomiao Cui, and Liefeng Bo. Mimo: Controllable character video synthesis with spatial decomposed modeling. *arXiv preprint arXiv:2409.16160*, 2024. 3
- [31] Maxime Oquab, Timothée Darcet, Théo Moutakanni, Huy Vo, Marc Szafranec, Vasil Khalidov, Pierre Fernandez, Daniel Haziza, Francisco Massa, Alaaeldin El-Nouby, et al. Dinov2: Learning robust visual features without supervision. *arXiv preprint arXiv:2304.07193*, 2023. 2, 4
- [32] Bohao Peng, Jian Wang, Yuechen Zhang, Wenbo Li, Ming-Chang Yang, and Jiaya Jia. Controlnext: Powerful and efficient control for image and video generation. *arXiv preprint arXiv:2408.06070*, 2024. 2, 3, 6, 7, 8
- [33] Alec Radford, Jong Wook Kim, Chris Hallacy, Aditya Ramesh, Gabriel Goh, Sandhini Agarwal, Girish Sastry, Amanda Askell, Pamela Mishkin, Jack Clark, et al. Learning transferable visual models from natural language supervision. In *International conference on machine learning*, pages 8748–8763. PmLR, 2021. 2, 4
- [34] Nikhila Ravi, Valentin Gabeur, Yuan-Ting Hu, Ronghang Hu, Chaitanya Ryali, Tengyu Ma, Haitham Khedr, Roman Rädle, Chloe Rolland, Laura Gustafson, et al. Sam 2: Segment anything in images and videos. *arXiv preprint arXiv:2408.00714*, 2024. 6
- [35] Aliaksandr Siarohin, Stéphane Lathuilière, Sergey Tulyakov, Elisa Ricci, and Nicu Sebe. First order motion model for image animation. *Advances in neural information processing systems*, 32, 2019. 3
- [36] Aliaksandr Siarohin, Oliver J Woodford, Jian Ren, Menglei Chai, and Sergey Tulyakov. Motion representations for articulated animation. In *Proceedings of the IEEE/CVF Conference on Computer Vision and Pattern Recognition*, pages 13653–13662, 2021. 6, 7
- [37] Gaurang Sriramanan, Siddhant Bharti, Vinu Sankar Sadasivan, Shoumik Saha, Priyatham Kattakinda, and Soheil Feizi. Llm-check: Investigating detection of hallucinations in large language models. In *Advances in Neural Information Processing Systems*, pages 34188–34216. Curran Associates, Inc., 2024. 3
- [38] Jianlin Su, Murtadha Ahmed, Yu Lu, Shengfeng Pan, Wen Bo, and Yunfeng Liu. Roformer: Enhanced transformer with rotary position embedding. *Neurocomputing*, 568:127063, 2024. 4
- [39] Ashkan Taghipour, Morteza Ghahremani, Mohammed Benamoun, Aref Miri Rekavandi, Hamid Laga, and Farid Boussaid. Box it to bind it: Unified layout control and attribute binding in t2i diffusion models. *arXiv preprint arXiv:2402.17910*, 2024. 3
- [40] Ashkan Taghipour, Morteza Ghahremani, Mohammed Benamoun, Aref Miri Rekavandi, Zinuo Li, Hamid Laga, and Farid Boussaid. Faster image2video generation: A closer look at clip image embedding’s impact on spatio-temporal cross-attentions. *arXiv preprint arXiv:2407.19205*, 2024. 3
- [41] Shuai Tan, Biao Gong, Xiang Wang, Shiwei Zhang, Dandan Zheng, Ruobing Zheng, Kecheng Zheng, Jingdong Chen, and Ming Yang. Animate-x: Universal character image animation with enhanced motion representation. *arXiv preprint arXiv:2410.10306*, 2024. 3
- [42] Shuyuan Tu, Zhen Xing, Xintong Han, Zhi-Qi Cheng, Qi Dai, Chong Luo, and Zuxuan Wu. Stableanimator: High-quality identity-preserving human image animation. *arXiv preprint arXiv:2411.17697*, 2024. 3, 4, 6, 7, 8
- [43] Thomas Unterthiner, Sjoerd Van Steenkiste, Karol Kurach, Raphael Marinier, Marcin Michalski, and Sylvain Gelly. To-

- wards accurate generative models of video: A new metric & challenges. *arXiv preprint arXiv:1812.01717*, 2018. 6
- [44] Jacob Walker, Ali Razavi, and Aäron van den Oord. Predicting video with vqvae. *arXiv preprint arXiv:2103.01950*, 2021. 3
- [45] Jiajun Wang, Morteza Ghahremani Boozandani, Yitong Li, Björn Ommer, and Christian Wachinger. Stable-pose: Leveraging transformers for pose-guided text-to-image generation. *Advances in Neural Information Processing Systems*, 37: 65670–65698, 2025. 3
- [46] Luozhou Wang, Yijun Li, Zhifei Chen, Jui-Hsien Wang, Zhifei Zhang, He Zhang, Zhe Lin, and Yingcong Chen. Transpixar: Advancing text-to-video generation with transparency. *arXiv preprint arXiv:2501.03006*, 2025. 2
- [47] Qilin Wang, Zhengkai Jiang, Chengming Xu, Jiangning Zhang, Yabiao Wang, Xinyi Zhang, Yun Cao, Weijian Cao, Chengjie Wang, and Yanwei Fu. Vividpose: Advancing stable video diffusion for realistic human image animation. *arXiv preprint arXiv:2405.18156*, 2024. 3
- [48] Tan Wang, Linjie Li, Kevin Lin, Yuanhao Zhai, Chung-Ching Lin, Zhengyuan Yang, Hanwang Zhang, Zicheng Liu, and Lijuan Wang. Disco: Disentangled control for realistic human dance generation. In *Proceedings of the IEEE/CVF Conference on Computer Vision and Pattern Recognition*, pages 9326–9336, 2024. 3, 6, 7
- [49] Xiang Wang, Shiwei Zhang, Changxin Gao, Jiayu Wang, Xiaoqiang Zhou, Yingya Zhang, Luxin Yan, and Nong Sang. Unianimate: Taming unified video diffusion models for consistent human image animation. *arXiv preprint arXiv:2406.01188*, 2024. 3, 4, 6, 7, 8
- [50] Yaohui WANG, Piotr Bilinski, Francois Bremond, and Antitza Dantcheva. Imaginator: Conditional spatio-temporal gan for video generation. In *Proceedings of the IEEE/CVF Winter Conference on Applications of Computer Vision (WACV)*, 2020. 3
- [51] Yaohui Wang, Piotr Bilinski, Francois Bremond, and Antitza Dantcheva. Imaginator: Conditional spatio-temporal gan for video generation. In *2020 IEEE Winter Conference on Applications of Computer Vision (WACV)*, pages 1149–1158, 2020. 3
- [52] Zhou Wang, A.C. Bovik, H.R. Sheikh, and E.P. Simoncelli. Image quality assessment: from error visibility to structural similarity. *IEEE Transactions on Image Processing*, 13(4): 600–612, 2004. 6
- [53] Zhao Wang, Hao Wen, Lingting Zhu, Chenming Shang, Yujiu Yang, and Qi Dou. Anycharv: Bootstrap controllable character video generation with fine-to-coarse guidance. *arXiv preprint arXiv:2502.08189*, 2025. 3
- [54] Haofei Xu, Jing Zhang, Jianfei Cai, Hamid Rezatofghi, Fisher Yu, Dacheng Tao, and Andreas Geiger. Unifying flow, stereo and depth estimation. *IEEE Transactions on Pattern Analysis and Machine Intelligence*, 45(11):13941–13958, 2023. 6
- [55] Jiaqi Xu, Xinyi Zou, Kunzhe Huang, Yunkuo Chen, Bo Liu, MengLi Cheng, Xing Shi, and Jun Huang. Easyanimate: A high-performance long video generation method based on transformer architecture. *arXiv preprint arXiv:2405.18991*, 2024. 2, 3
- [56] Zhongcong Xu, Jianfeng Zhang, Jun Hao Liew, Hanshu Yan, Jia-Wei Liu, Chenxu Zhang, Jiashi Feng, and Mike Zheng Shou. Magicanimate: Temporally consistent human image animation using diffusion model. In *Proceedings of the IEEE/CVF Conference on Computer Vision and Pattern Recognition*, pages 1481–1490, 2024. 3, 6, 7
- [57] Wilson Yan, Yunzhi Zhang, Pieter Abbeel, and Aravind Srinivas. Videogpt: Video generation using vq-vae and transformers. *arXiv preprint arXiv:2104.10157*, 2021. 3
- [58] Lihe Yang, Bingyi Kang, Zilong Huang, Zhen Zhao, Xiaogang Xu, Jiashi Feng, and Hengshuang Zhao. Depth anything v2. *arXiv preprint arXiv:2406.09414*, 2024. 3, 6
- [59] Zhendong Yang, Ailing Zeng, Chun Yuan, and Yu Li. Effective whole-body pose estimation with two-stages distillation. In *Proceedings of the IEEE/CVF International Conference on Computer Vision*, pages 4210–4220, 2023. 3
- [60] Zhuoyi Yang, Jiayan Teng, Wendi Zheng, Ming Ding, Shiyu Huang, Jiazheng Xu, Yuanming Yang, Wenyi Hong, Xiaohan Zhang, Guanyu Feng, et al. Cogvideox: Text-to-video diffusion models with an expert transformer. *arXiv preprint arXiv:2408.06072*, 2024. 2
- [61] Zhuoyi Yang, Jiayan Teng, Wendi Zheng, Ming Ding, Shiyu Huang, Jiazheng Xu, Yuanming Yang, Wenyi Hong, Xiaohan Zhang, Guanyu Feng, et al. Cogvideox: Text-to-video diffusion models with an expert transformer. *arXiv preprint arXiv:2408.06072*, 2024. 2, 3, 4, 5
- [62] Shenghai Yuan, Jinfa Huang, Xianyi He, Yunyuan Ge, Yujun Shi, Liuhan Chen, Jiebo Luo, and Li Yuan. Identity-preserving text-to-video generation by frequency decomposition. *arXiv preprint arXiv:2411.17440*, 2024. 2
- [63] Jieyu Zhang, Weikai Huang, Zixian Ma, Oscar Michel, Dong He, Tanmay Gupta, Wei-Chiu Ma, Ali Farhadi, Aniruddha Kembhavi, and Ranjay Krishna. Task me anything. In *Advances in Neural Information Processing Systems*, pages 19965–19974. Curran Associates, Inc., 2024. 3
- [64] Lvmin Zhang, Anyi Rao, and Maneesh Agrawala. Adding conditional control to text-to-image diffusion models. In *Proceedings of the IEEE/CVF international conference on computer vision*, pages 3836–3847, 2023. 5
- [65] Richard Zhang, Phillip Isola, Alexei A. Efros, Eli Shechtman, and Oliver Wang. The unreasonable effectiveness of deep features as a perceptual metric. *2018 IEEE/CVF Conference on Computer Vision and Pattern Recognition*, pages 586–595, 2018. 6
- [66] Yang Zhang, Jiayi Gu, Li-Wen Wang, Han Wang, Junqi Cheng, Yuefeng Zhu, and Fangyuan Zou. Mimicmotion: High-quality human motion video generation with confidence-aware pose guidance. *arXiv preprint arXiv:2406.19680*, 2024. 3, 4, 6, 7
- [67] Yuhang Zhang, Yuan Zhou, Zeyu Liu, Yuxuan Cai, Qiuyue Wang, Aidong Men, and Huan Yang. Fleximo: Towards flexible text-to-human motion video generation. *arXiv preprint arXiv:2411.19459*, 2024. 3
- [68] Zangwei Zheng, Xiangyu Peng, Tianji Yang, Chenhui Shen, Shenggui Li, Hongxin Liu, Yukun Zhou, Tianyi Li, and Yang You. Open-sora: Democratizing efficient video production for all. *arXiv preprint arXiv:2412.20404*, 2024. 3

- [69] Zhengguang Zhou, Jing Li, Huaxia Li, Nemo Chen, and Xu Tang. Storymaker: Towards holistic consistent characters in text-to-image generation. *arXiv preprint arXiv:2409.12576*, 2024. [3](#)
- [70] Shenhao Zhu, Junming Leo Chen, Zuozhuo Dai, Zilong Dong, Yinghui Xu, Xun Cao, Yao Yao, Hao Zhu, and Siyu Zhu. Champ: Controllable and consistent human image animation with 3d parametric guidance. In *European Conference on Computer Vision*, pages 145–162. Springer, 2025. [1](#), [3](#), [4](#), [6](#), [7](#), [8](#)